

Cycle Slip Detection in Galileo Widelane Signals Tracking

Philippe Paimblanc, *TéSA*
Nabil Jardak, *M3 Systems*
Margaux Bouilhac, *M3 Systems*
Thomas Junique, *CNES*
Thierry Robert, *CNES*

BIOGRAPHIES

Philippe PAIMBLANC graduated as electronics engineer from the ENAC (Ecole Nationale de l'Aviation Civile) in 2002 and received the same year his Master research degree in signal processing. He performed a PhD at the satellite navigation lab of the ENAC. He is now a research engineer at TéSA laboratory, in Toulouse, France. His research activity is centered on satellite navigation and positioning.

Nabil JARDAK: PhD in Radio-navigation from TELECOM-INT/UPMC Paris VI (2008) and telecommunication engineer from Sup'Com Tunis (2005), he joined in 2009 the Radio-navigation Unit of M3 Systems as Radio-navigation and signal processing engineer. Since then, he is involved in many activities covering land, space and scientific applications of GNSS where he worked in particular on GNSS algorithm design and has developed advanced simulators for the prediction of GNSS system's performance in constrained environments. Since 2017, Nabil is head of the Radionavigation Unit at M3 Systems.

Margaux BOUILHAC has been graduated as telecom and network engineer from ENSEEIHT, Toulouse, France in 2015. Since then, she has been working as a radio-navigation and signal processing engineer in M3 Systems. For M3 Systems and in collaboration with CNES, the french space agency, she is involved in many activities including GNSS algorithm design and GNSS performances analysis.

Since March 2012, Thomas JUNIQUE has been working as a radio-navigation engineer in Signals and Equipment Radio-navigation/radio-localization department of the CNES. He works on research and development on spatial GNSS receivers. In this activity, he has worked on the MICROSCOPE satellite for two years. Moreover, he is responsible of the navigation laboratory in CNES and also manages activities concerning terrestrial receivers (algorithms); especially in integrity field. Prior to joining the CNES, he worked 2 years in a private company, M3 Systems, carrying out some research activities in the CNES navigation laboratory. He graduated from "Ecole Nationale de l'Aviation Civile" ENAC, in Toulouse (FRANCE) in 2009.

Thierry ROBERT received the Ph.D. degree from National Polytechnic Institute of Toulouse in 1996. He is currently the Head of the Location/Navigation Signal and Time Frequency Department, Centre national d'études spatiales (CNES)—the French Space Agency. The department's activities cover signal design and processing, receivers and payloads involving location, and navigation systems including GNSS (Galileo and GNSS space receivers), search and rescue by satellite (Cospas-Sarsat and MEOSAR), and Argos. Other activities covered by the department is the time and frequency reference generation including the UTC (CNES) generation.

ABSTRACT

Precise positioning (based on Precise Point Positioning, PPP, or Real Time Kinematics, RTK) is steadily gaining momentum. The main difficulty when using carrier phase measurements remains to correctly estimate their ambiguities: not only is it a computationally intensive process, but it can be affected by cycle slips (CS), which are brutal variations in ambiguity values, due to receiver's dynamics or unfortunate reception events. As GNSS constellations are now able to provide users with signals on three different frequencies, the concept of Triple Carrier Ambiguity Resolution has become widespread. It typically relies on the use of widelane signals, which are combinations of raw signals and are defined as to have an apparent wavelength much higher than original signals, thus making accelerating the ambiguity fixing process and reducing the frequency of cycle slips. However, CS may remain a problem for the availability of precise positioning services. The present paper therefore focuses on a cycle slip detection method, based on a hypothesis test. The main idea consists in using both code and widelane phase

measurements to compute a geometry- and ionospheric-free test vector, theoretically containing only noise and possible cycle slips. The latter can be detected by looking for brutal changes on the average of the test vector. Performance is assessed on simulated and Rinex data.

INTRODUCTION

The Galileo satellite positioning system currently provides signals on three different bands: E1, E5 and E6, which have respective central frequencies of 1575.42 MHz, 1191.795 MHz and 1278.75 MHz, as illustrated in Figure 1. In particular, the signal broadcasted on E5 is an AltBOC(15,10), characterized, among other features, by its relatively large bandwidth. One of the outcomes of this feature is that the E5 phase tracking is comparatively more stable than E1 and E6. As a result, the frequency of cycle slips is lower for E5 than for other signals.

A patented tracking device [1] was developed to take advantage of this: its main principle consisted in first taking the AltBOC E5 phase as a reference and then tracking widelane linear combinations of E5 and E1, and E5 and E6: W51 and W56.

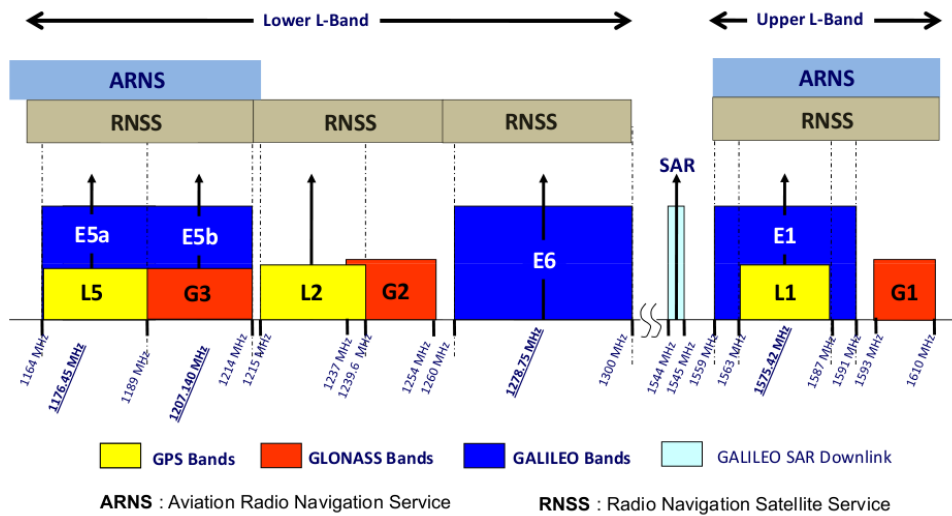


Figure 1: GNSS navigation bands, from Navipedia

WIDELANE MULTI-FREQUENCY TRACKING

As presented in the introduction, widelane signals are linear combinations of two raw signals. They are obtained by multiplying the correlator outputs from one raw signal (typically E1 or E6) with the correlator outputs from another raw signal (typically E5). The principle is illustrated in Figure 2.

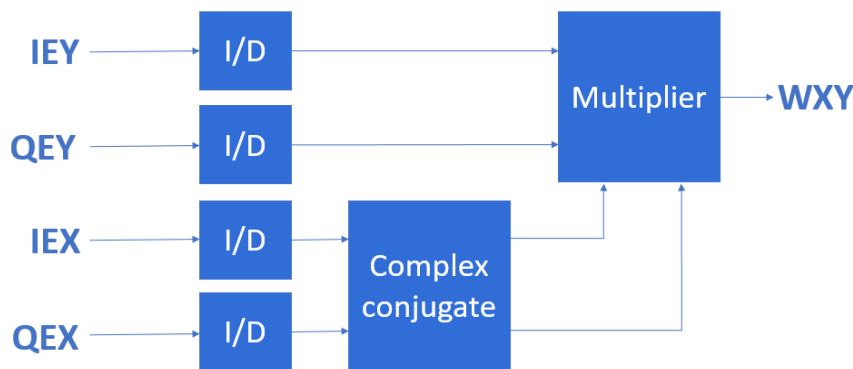


Figure 2: Generation of widelane signals

In the case of E5 and E1, the widelane phase combination is expressed as:

$$\Phi_w = \Phi_{E1} - \Phi_{E5} = \frac{f_w}{c} \rho + N_w + f_w \Delta \delta - \left(\frac{1}{\lambda_{E1}} \Delta_{iono}(f_{E1}) - \frac{1}{\lambda_{E5}} \Delta_{iono}(f_{E5}) \right)$$

where:

- $\Phi_{E1} = \frac{f_{E1}}{c} \rho + N_{E1} + f_{E1} \Delta\delta - \frac{1}{\lambda_{E1}} \Delta^{iono}(f_{E1})$, E1 phase,
- $\Phi_{E5} = \frac{f_{E5}}{c} \rho + N_{E5} + f_{E5} \Delta\delta - \frac{1}{\lambda_{E5}} \Delta^{iono}(f_{E5})$, E5 phase
- $N_w = N_{E1} - N_{E5}$, ambiguity of the composite signal,
- c : celerity of light,
- ρ : pseudo-range,
- $\Delta\delta$: satellite and receiver clock bias.

This W51 composite signal has an apparent frequency in the order of a hundred MHz, and its wavelength is around 30 centimeters. W51 is therefore considerably less subject to cycle slips than E1.

The tracking architecture is based on a Kalman filter and is illustrated in Figure 3.



Figure 3: Kalman-based tracking architecture

The outputs of this tracking system are:

- ρ_τ , the code pseudo-range measured on E5, unambiguous but noisy,
- φ_{51} , the carrier phase measurement on the widelane signal W51,
- φ_{56} , the carrier phase measurement on the widelane signal W56,
- φ_{E5} , the carrier phase measurement on E5.

These outputs share some properties with measurements obtained through more classical method, in particular that ρ_τ is unambiguous but noisy, while the phase measurements are ambiguous and occasionally affected by cycle slips, but display a much lower noise level.

However, the widelane signals have an original characteristic: it is that, due to their large wavelength, the amplitude of the cycle slips is high as compared to noise levels. Indeed, the wavelength of the widelane signal W56 is equal to $c/(f_{E6} - f_{E5}) = 3.45\text{m}$. Since this wavelength is significantly higher than expected standard deviation values on E5 code measurement, it means that ρ_τ can be used as a reference signal to detect possible cycle slips on W56. $c/(f_{E6} - f_{E5}) = 3.45\text{m}$ In fact, a cascading detection algorithm could be envisaged, as illustrated in : W56 phase measurements are tested by comparing them to E5 code measurements; when (and if) they are cleared, they can be used as reference to test W51 phase measurements, since their standard deviation is expected to be significantly lower than the 78 cm wavelength of W51 signals. Finally, if declared free from any cycle slip, W51 phase signals can be used to test the presence of cycle slips on E5. The actual test is described in the following section.

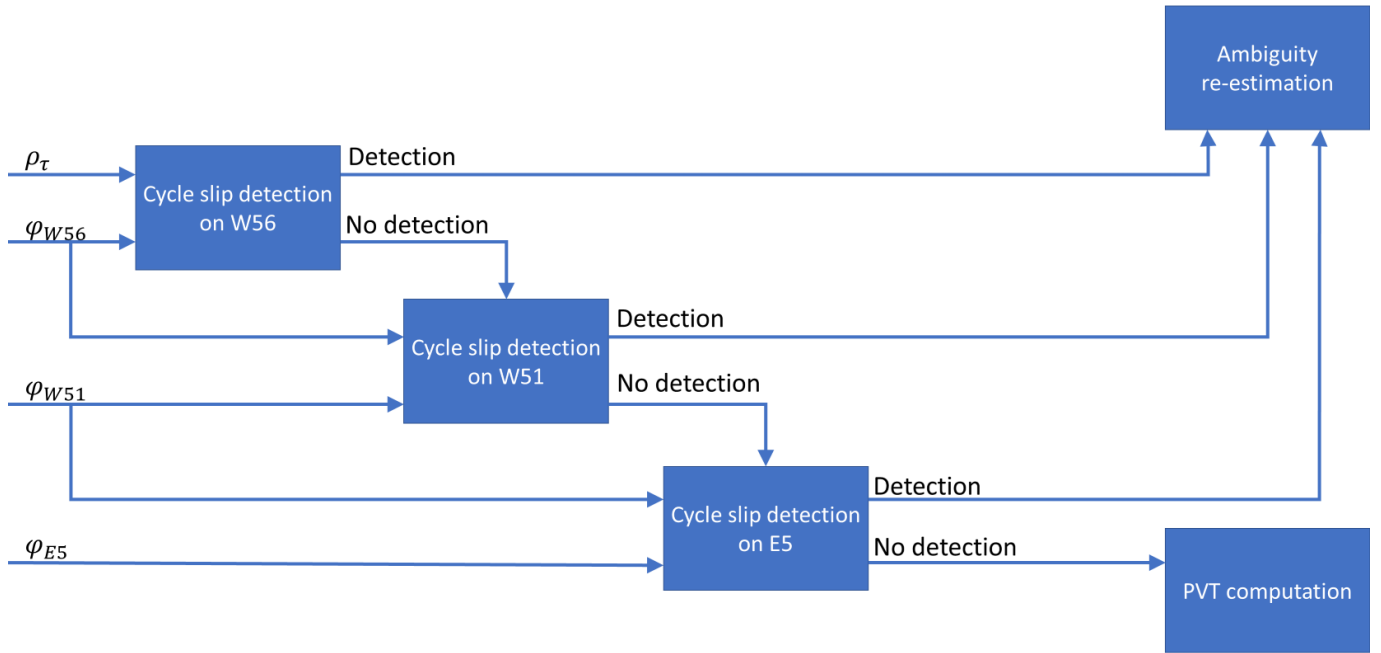


Figure 4: structure of the cascading cycle slip detection algorithm.

CYCLE SLIP DETECTION TEST

The first step is to generate a test variable based on the reference measurement and the tested phase measurement. In the case of the W56 signal, it can be performed as follows. First, the code-phase difference is formed:

$$\rho\varphi_{56} = \rho_{\tau} - \varphi_{56}.$$

Then, to limit the impact of the ionospheric bias, the variable is differenced over time:

$$\delta\rho\varphi_{56}^{(n)} = \rho\varphi_{56}^{(n)} - \rho\varphi_{56}^{(n-K)},$$

Where $\delta\rho\varphi_{56}^{(n)}$ is the code-phase difference at current epoch n and $\rho\varphi_{56}^{(n-K)}$ the code-phase difference at reference epoch $n - K$. K is an integer parameter that defines the length of the observation window. Indeed, $\delta\rho\varphi_{56}^{(n)}$ is a random variable that has zero average if no cycle slip occurred between n and $n - K$. Otherwise, if a cycle slip has indeed occurred, an abrupt change in the average of $\delta\rho\varphi_{56}^{(n)}$ will be observed. Additionally, the new average will be equal to the amplitude of the CS.

Two different tests have been implemented. The first one consists in performing a hypothesis test on the possible values of the new mean in case of a cycle slip. Indeed, assuming that the cycle slips have a limited amplitude, the mean of $\delta\rho\varphi_{56}^{(n)}$ can only take a finite number of integer values: $\{-N, \dots, +N\}$. Each value in $\{-N, \dots, +N\}$ can therefore be considered as a hypothesis whose likelihood can be tested over the length of the observation window.

$\delta\rho\varphi_{56}^{(n)}$ is assumed to follow a Gaussian distribution with mean m and variance σ^2 . The variance is assumed to be unknown and the mean can take any of the known $2N + 1$ values in $\{-N, \dots, +N\}$, corresponding to the amplitude of the cycle slip. The principle of the proposed algorithm consists in performing $2N + 1$ hypothesis tests in parallel, to determine the value of m , and, for each possible value m_k , to choose between the two following hypotheses:

$$H_k: m = m_k \quad \bar{H}_k: m \neq m_k$$

In a first approach, the test statistic ought to be the empirical mean:

$$\overline{\delta\rho\varphi} = \frac{1}{K} \sum_{n=1}^K \delta\rho\varphi_{56}^{(n)}$$

$\overline{\delta\rho\varphi}$ follows a Gaussian distribution with mean m and variance σ^2/K . As σ^2 is unknown, it can be approached using the empirical variance S^2 , defined as:

$$S^2 = \frac{1}{K-1} \sum_{n=1}^K (\delta\rho\varphi_{56}^{(n)} - \overline{\delta\rho\varphi})^2.$$

Under hypothesis H_k , the following variable:

$$T_k = \frac{\overline{\delta\rho\varphi} - m_k}{S/\sqrt{K}}$$

Follows a Student law with $(K-1)$ degrees of freedom [1].

Thus, the test called bi-lateral Student test [1] is based on the following rule:

$$\text{Rejection of } H_k \Leftrightarrow |(T_k)_{obs}| \geq \mu_\alpha,$$

Where $(T_k)_{obs}$ is the observed value of test statistic T_k and μ_α the value of the threshold computed from the false alarm probability:

$$\alpha = 2P[T_k \geq \mu_\alpha | T_k \text{ follows } t_{K-1}],$$

as illustrated in Figure 5.

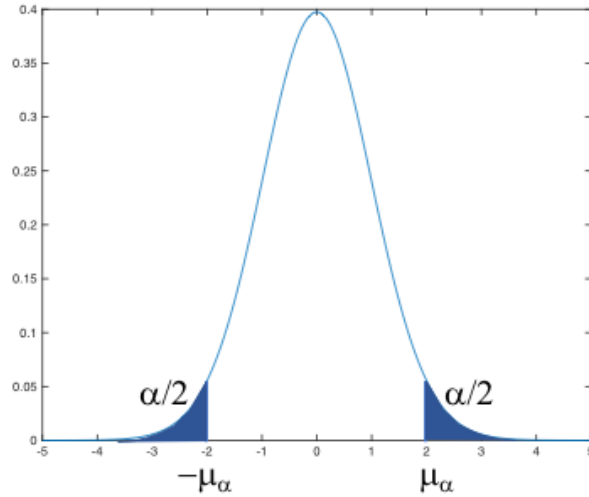


Figure 5: Distribution of test statistic T_k under H_k

Typical values for α are 1% or 5%.

However, in the present case, the student test cannot be directly applied. Indeed, performing $2N + 1$ tests in parallel, over the $2N + 1$ possible values for m : if the standard deviation σ is small enough as compared to the interval between two possible values of m , the $2N + 1$ tests will provide $2N$ rejection decisions and only one non-rejection decision. In the opposite case, one could end with several no-rejection decisions, making it impossible to conclude on the value of m .

In the latter case, the test cannot be used as a decision rule but rather according to Fisher theory [1], which associates the null hypothesis H_k with a p -value defined as:

$$p_k = P[|T_k| \geq (T_k)_{obs} | T_k \text{ follows } t_{K-1}].$$

The p -value is the probability under H_k to obtain a statistic as large as the observed value. It can be interpreted as the smallest significance level for which the H_k hypothesis is accepted, or as a measure of how much observed data suggest the rejection of H_k . However, it is *not* the probability for H_k to be true.

Thus, in the present case, the $2N + 1$ Student tests performed in parallel are associated with their p -values: the chosen H_k hypothesis is the one with the highest p -value: it is the one for which the data give the smallest suggestion for rejection.

In practice, the Student test is applied at each epoch to a vector of data collected over an observation window of length K . For instance, for variable $\delta\rho\varphi_{56}$, the collected vector is:

$$\delta\rho\varphi_{56}^{(n-K+1)}, \dots, \delta\rho\varphi_{56}^{(n)}.$$

The bi-lateral Student test is applied to this measurement vector, in order to determine the likeliest mean: all the hypotheses from the $\{-N, \dots, +N\}$ domain are tested, the one with the highest p -value is considered the likeliest. If the estimated mean is non-zero, a cycle slip has occurred.

To avoid having too many false alarms, the results of the Student tests are accumulated over a second observation window, of length K_D . This operation provides a vector containing the likeliest mean over K_D consecutive samples: $m^{(n-K_D+1)}, \dots, m^{(n)}$. This vector is used to make sure empirically that the mean computation process is consistent over time. To do this, the most frequent value of m in the vector is determined, as well as the number of its occurrences. If this number is higher than a parameterizable threshold, and the corresponding value non-zero, a cycle slip is detected. Otherwise, the test was not conclusive.

The Student test is not originally designed to detect a change in mean. Examples of algorithms designed to detect abrupt changes in time series can be found in [3], such as the classic generalized likelihood ratio-based cumulative sum algorithm (GLR-CUSUM). However, [5] proposes to use the Kiefer-Wolfowitz algorithm (introduced in [4]) because of its lower complexity and lower false alarm rate. [5] also shows that, when detecting abrupt changes in the mean of Gaussian variables, the KW-CUSUM algorithm is equivalent to a moving average. Thus, the algorithm that was tested consists in computing, at every epoch n , the integer closest to the empirical mean of $\delta\rho\varphi_{56}^{(n)}$:

$$m^{(n)} = \text{round} \left(\frac{1}{K} \sum_{i=0}^{K-1} \delta\rho\varphi^{(n-i)} \right)$$

Simulation results for both methods are presented in the next section.

PERFORMANCE ASSESSMENT

Synthetic signals

The performance of the two algorithms have been assessed both in terms of false alarm and missed detection rates, under the following conditions:

- The tracking filter is single-channel, and the detection test is single frequency,
- The input data are the unambiguous reference measurements and the phase measurements,
- Tested cycle slip amplitude belongs to the $\{-10; 10\}$ interval,
- For the Student test, the observation window contains 50 samples, the decision window contains 10 samples, $\{-10; 10\}$ and the decision threshold is 3,
- For the moving average test, the observation window contains 50 samples (no decision window was used),
- Simulations are performed on a minimum of 10^5 tests per standard deviation value, and go on until 100 events (false alarm or missed detection) have been registered.

False alarm results are illustrated in Figure 6 for both methods. False alarm refers to the detection of a cycle slip when ambiguity has in fact remained constant. FA rates are provided with regards to the standard deviation of unambiguous reference measurements. Standard deviation is expressed as a percentage of the wavelength, which illustrates the fact that, reception conditions remaining otherwise constant, a cycle slip will be easier to detect if the wavelength is higher. Therefore, even if phase measurements are processed one frequency at a time, it benefits greatly from being applied to widelane signals.

False alarm rates tend to increase rapidly when standard deviation increases. It must however be noted that E5 code measurements are only used to test widelane W56 signals, whose wavelength is 3.44m. In typical reception conditions, E5 code standard deviations are expected to be lower than 0.5λ . Indeed, for a standard deviation equal to 20 % of the wavelength, the Student method provides an FA rate around 2×10^{-5} . As for the moving average method, FA rates are lower than 10^{-9} for any standard deviation inferior to 30% of the wavelength (approximately 1 meter).

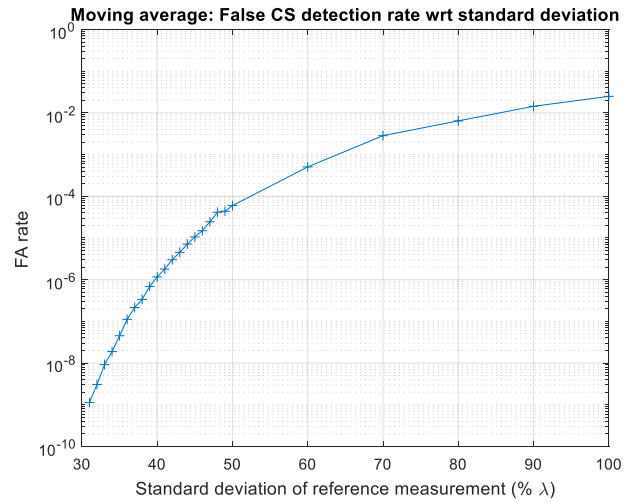
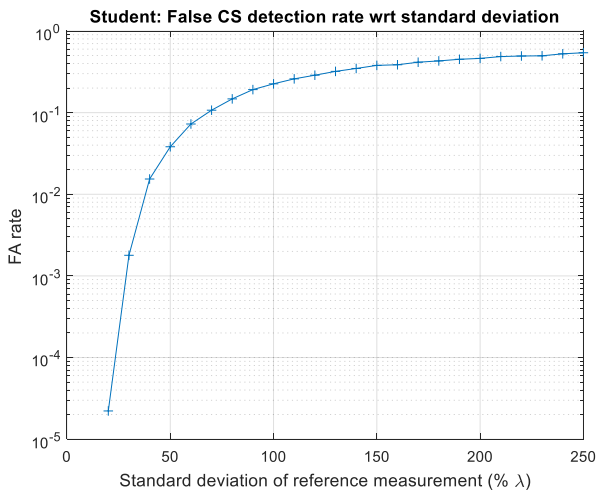


Figure 6: False cycle slip detection rate for the Student and moving average methods

Missed detection results are presented in Figure 7. Since the distribution of cycle slip amplitude is not a priori known, a worst-case scenario has been used, where generated cycle slips have an amplitude of only one wavelength, even though all hypotheses in the $\{-10; 10\}$ interval are tested. Once again, the moving average method is considerably more efficient than the Student method.

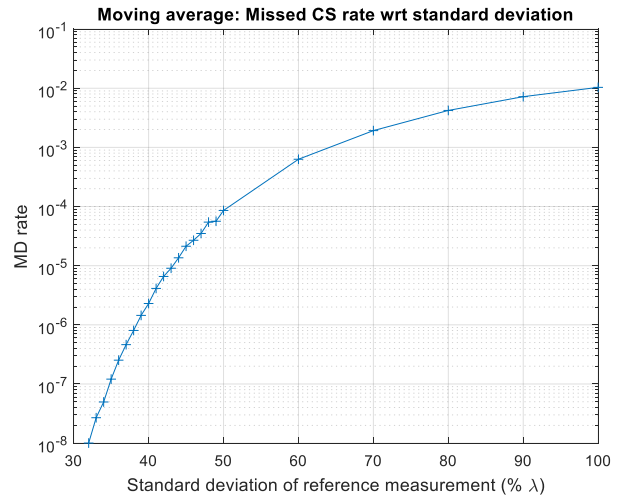
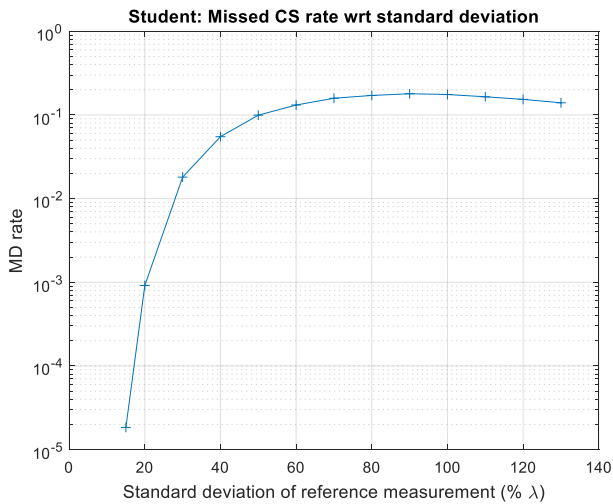


Figure 7: Missed cycle slip detection rate for the Student and moving average methods

Unfortunately, even though the moving average method is the most interesting, both in terms of raw performance and computational complexity, only the Student-based method was tested on real data during the study.

RINEX data

To test the cycle slip detection function in more realistic conditions, the algorithm was implemented to work with Rinex data files. It includes three main functions:

- Cascading CS detection, as described above,
- Cascading integer ambiguity fixing,
- RTK PVT computation.

The RTK PVT computation was performed using data from two close Rinex stations (TLSE and TL5G), taking one as reference and the other as rover. For data availability reasons, the analysis was performed on GPS L1, L2 and L5. L5 signals were used as reference for the computation of widelane signals WL52 and WL51.

The chosen performance criterion is the PVT error for each of the three signals. The different PVT solutions are computed in three steps:

1. First, the ambiguity fixing method is applied to ρ_5 and φ_{52} . The wavelength for this step is approximately 5.86m,
2. Next, the ambiguity is fixed using φ_{52} and φ_{51} , associated with a 0.5 cm wavelength,
3. Finally, ambiguity fixing is performed on φ_{51} and φ_5 .

The following figures compare the PVT errors obtained with the three frequencies with float and integer ambiguity fixing. On the left, the CS detection algorithm was used before ambiguity fixing. On the right, ambiguity and PVT were computed without CS detection.

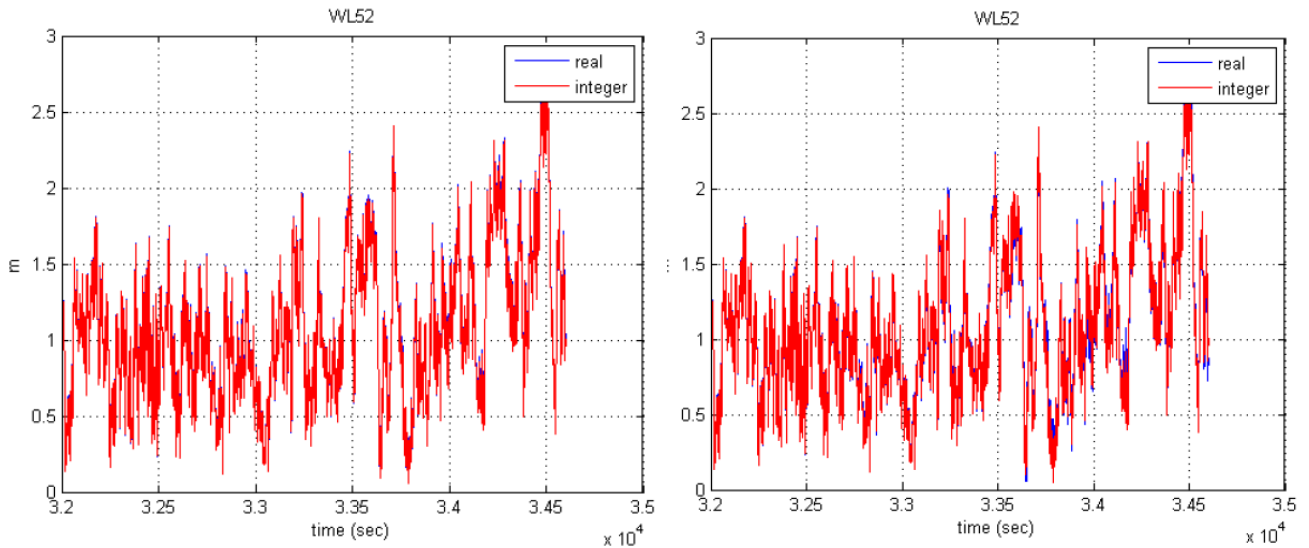


Figure 8: PVT error on WL52, with and without CS detection

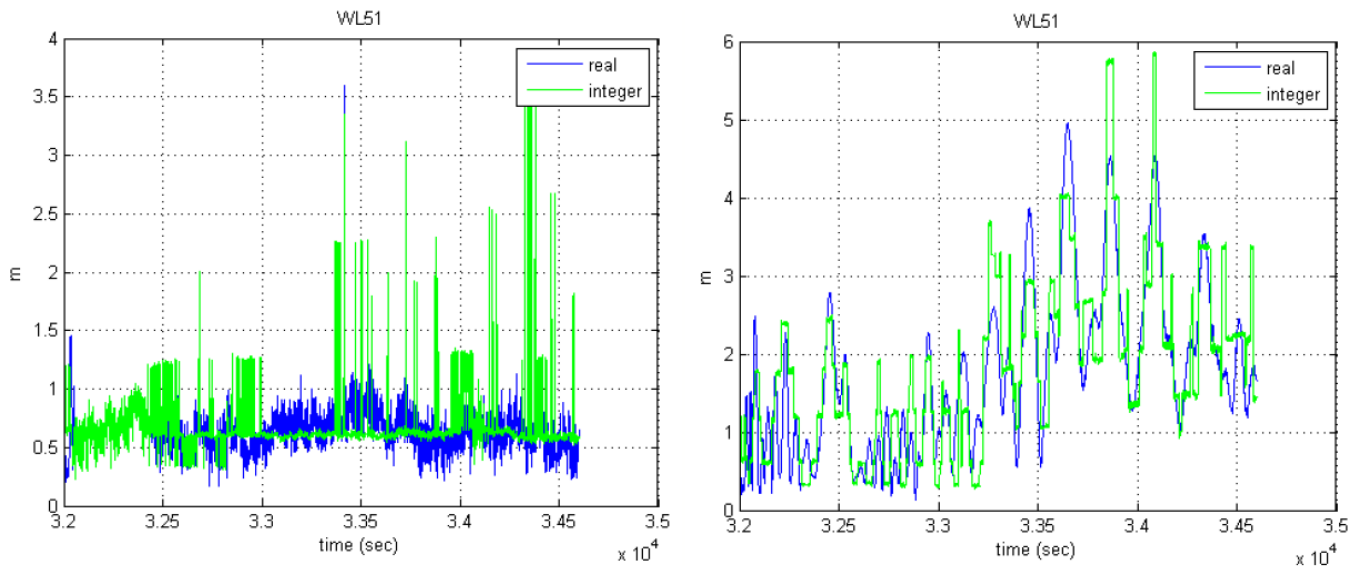


Figure 9: PVT error on WL51, with and without CS detection

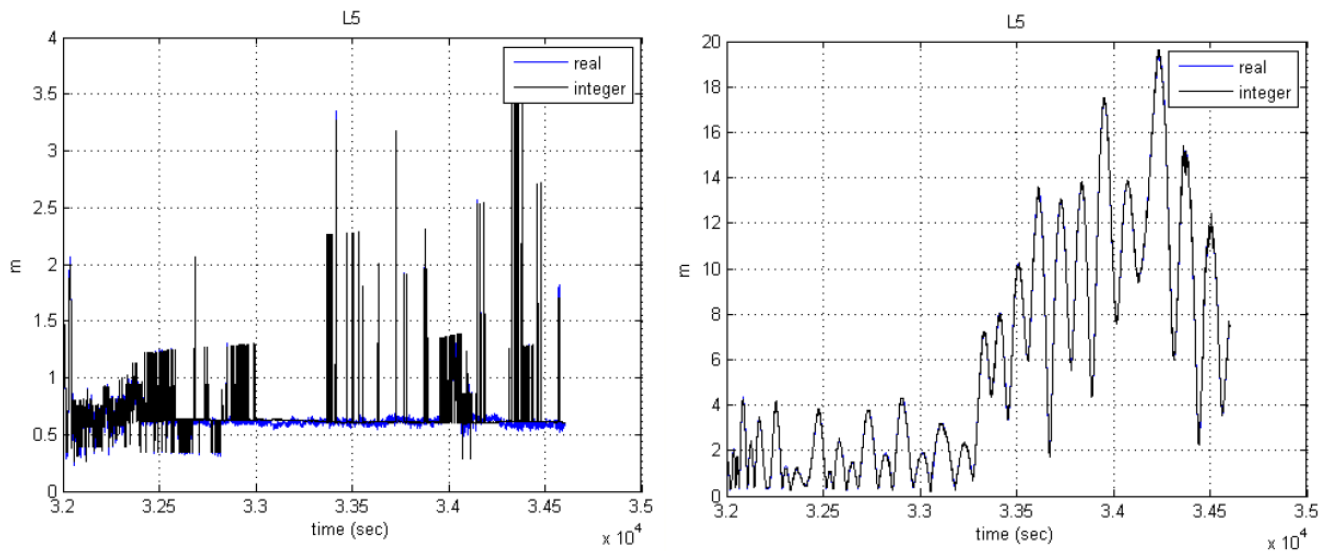


Figure 10: PVT error on WL5, with and without CS detection

Although the first step is very little impacted by the presence or absence of a CS detection test, the outputs of steps 2 and 3 clearly show a divergence of PVT errors on WL51 and L5. This proves the relevance of performing a channel-level cycle slip detection test, in order to prevent ambiguity fixing algorithms from diverging.

CONCLUSION

A multi-frequency phase tracking method has previously been developed and patented by the CNES. Based on the computation of widelane signals, it is characterized by more reliable phase measurements, due to the lower frequency of cycle slips, thus increasing the availability of precise positioning methods.

In order to further increase the reliability of the phase measurements, two cycle slips detection methods have been developed. The algorithms themselves are quite simple, but they owe their efficiency to the input signals: the large wavelengths of the widelane signals (W56 in particular) make it possible to detect a cycle slip using E5 code measurements as primary unambiguous measurements. Thanks to a cascading detection scheme, it is possible to use W51 phase measurements (once they have been checked) to monitor E5 phase measurements.

Simulation results were confirmed by tests on Rinex GPS data.

ACKNOWLEDGMENTS

The work presented in this paper has been performed thanks to CNES funding.

REFERENCES

- [1] Jardak N., Paimblanc P., Puengnim A., Ries L. & Vigneau W., Radionavigation signals tracking device, patent n°FR 3000806, January 2013, international extension in July 2014
- [2] Lehmann, E. L., & Romano J. P., *Testing Statistical Hypotheses (3E ed.)*. New York: Springer, 2005
- [3] Basseville, M., & Nikiforov, I. V., *Detection of abrupt changes: theory and application (Vol. 104)*. Englewood Cliffs: Prentice Hall, 1993
- [4] Kiefer, J., & Wolfowitz, J., *Stochastic estimation of the maximum of a regression function*. The Annals of Mathematical Statistics, 23(3), 462-466, 1952

- [5] Singamasetty, V., Nair, N., Bhashyam, S., & Kannu, A. P., *Change detection with unknown post-change parameter using Kiefer-Wolfowitz method*. In Acoustics, Speech and Signal Processing (ICASSP), 2017 IEEE International Conference on (pp. 3919-3923). IEEE, March 2017.